The rotor spinning process for fibre production

P. den Decker, H. Knoester, H. Meerman[†], K. Dekker, W. van Horssen, C. Vuik, P. Wesseling[‡], G. Prokert[§], B. van 't Hof[♯], F. van Beckum[♯]

1. Introduction

At Tejin Twaron in Arnhem new ways of producing fibres are being developed. One of the interesting techniques is the so-called Rotor Spinning Process. In principle, this process looks a lot like the making of sugarflos (or cotton candy) at a fair. Here, however, we deal with a polymer-filled disc with tiny holes. The polymer is pressed, due to the centrifugal forces, through the holes to the outside. This process is already in operation at the company; at Tejin Twaron there is also a pilot machine in which variations in the process and geometry can be tested.
The liquid polymer solidifies and becomes a thin filament on the exterior boundary of the machine. The purpose of the work during the week "Mathematics with Industry" is to verify an existing model on the basis of a momentum equation and mass balance and if possible to improve the model.
A first order approximation of the path of the filament (without modelling air friction) in the space between disc and exterior boundary of the machine exists already. Also a description of the path with water cooling and air friction is available. However, the model can be improved: certain states of the rotor spin process should be approximated in a better way. The ultimate purpose of the modelling in more detail reads:

1 Try to describe the situation (process and geometry) in which continuous filaments can be generated. Breaking of filaments may cause problems in the use of the material if the length of the filament is below a critical length.
2 Try to determine the circumstances (process and geometry) in which the length of a broken filament can be determined beforehand. In this case fibres can, in principle, be produced.
3 Determine the effect of processing conditions (e.g. temperature, rotor speed) in the present operating situation in order to achieve a robust production process.

During the workshop we mainly focused on the existing model used at Tejin Twaron, a boundary-value problem for differential equations, which is described in Section 2. As shooting techniques from the NAG-library did not yield acceptable results at Tejin Twaron, we considered the model from various perspectives. One subgroup tried to solve the model numerically, using MATLAB, by Picard-iteration starting from a model without viscosity. A second subgroup analyzed the model using perturbation theory in the neighborhood of the orifice and the last subgroup derived a time-dependent description including an energy balance. Their results are presented in the subsequent sections. Finally we present our conclusions and ideas for further research.

2. The mathematical model

A disc with radius R_{rot} is rotating anti-clockwise with angular velocity ω. The polymer (density ρ and viscosity η) is extruded from an orifice, and subsequently moves in the direction of the coagulator, which has radius R_{coag}. In a stable stationary process the trajectory of the polymer, the so-called spinning line, will be fixed in a rotating coordinate system. Therefore, we omit the time-derivatives in the model, but consider the movement of the polymer along the spinning line (see Fig. 1). Then, the independent variable is s, the arc-length along the

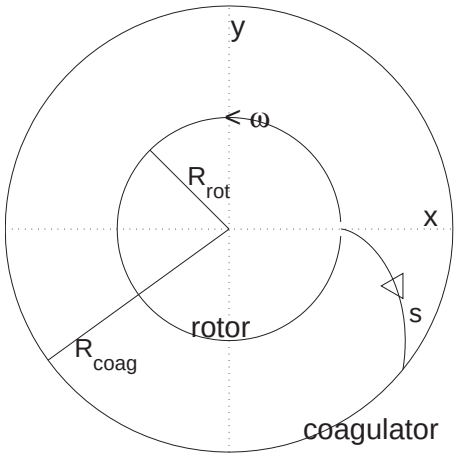

FIGURE 1. Spinning line in rotating coordinate system

spinning line, and the dependent variables are the position x, y of the spinning line, the velocity v of the polymer along the spinning line, and the diameter A of the spinning line. The variables x, y, s satisfy the equation

$$\left(\frac{dx}{ds}\right)^2 + \left(\frac{dy}{ds}\right)^2 = 1, \tag{1}$$

and the balance of mass gives a relation between A and v, as the mass flux Φ should be constant:

$$\rho A v = \Phi.$$

In the simple model without air friction we consider the viscous forces, the centrifugal force and the Coriolis force acting on an element of the spinning line of size Δs and position x, y:

$$\begin{aligned}
\mathbf{F}_{centr} &= \Delta s\, \rho A \omega^2 \begin{bmatrix} x \\ y \end{bmatrix}, \\
\mathbf{F}_{cor} &= 2\Delta s\, \rho A \omega v \begin{bmatrix} \frac{dy}{ds} \\ -\frac{dx}{ds} \end{bmatrix}, \\
\mathbf{F}_{visc} &= \Delta s \begin{bmatrix} \frac{d}{ds}\left(F\frac{dx}{ds}\right) \\ \frac{d}{ds}\left(F\frac{dy}{ds}\right) \end{bmatrix}.
\end{aligned}$$

Here, F denotes the norm of the viscous force vector at s. Balance of momentum then leads to the second order differential equations

$$(F - \Phi v)\frac{d^2x}{ds^2} = -\frac{\Phi\omega^2 x}{v} - 2\Phi\omega\frac{dy}{ds} - \frac{dx}{ds}\frac{d}{ds}(F - \Phi v), \tag{2}$$

$$(F - \Phi v)\frac{d^2y}{ds^2} = -\frac{\Phi\omega^2 y}{v} + 2\Phi\omega\frac{dx}{ds} - \frac{dy}{ds}\frac{d}{ds}(F - \Phi v). \tag{3}$$

Further it is assumed that the polymer is Newtonian, so the viscous force satisfies

$$\frac{dv}{ds} = \frac{\rho v}{\eta}\frac{F}{\Phi}. \tag{4}$$

Instead of solving the differential equations (2-4), together with the algebraic condition (1), it seemed more appropriate to replace (1) by a differential equation. Taking the inner product of vectorial momentum equations (2-3) and the vector

$$\left(\frac{dx}{ds}, \frac{dy}{ds}\right)^T,$$

using (1) and its differentiated form, leads to

$$\frac{dF}{ds} = \Phi\frac{dv}{ds} - \frac{\Phi\omega^2}{v}\left(x\frac{dx}{ds} + y\frac{dy}{ds}\right). \tag{5}$$

The initial conditions for the system (2-5) are

$$x(0) = R_{rot}, \quad y(0) = 0, \quad v(0) = v_0, \quad F(0) = F_0, \tag{6a}$$

$$\frac{dx}{ds} = 1, \quad \frac{dy}{ds} = 0, \quad \text{for } s = 0. \tag{6b}$$

The viscous force F_0 is unknown and should follow from conditions imposed on the spinning line at the coagulator. As the arc length L of the

spinning line at the coagulator is still unknown, we need two boundary conditions. The first one is given by the radius of the coagulator; moreover the velocity of the spinning line is assumed to be known:

$$x(L)^2 + y(L)^2 = R_{coag}, \quad v(L) = v_e.$$

It is easy to solve these equations in case of zero viscosity. Then, the model reduces to the problem of bullets fired from a rotating disc. Obviously, they move in a straight line, and the solution in a rotating coordinate system is given by

$$x(t) = (R_{rot} + v_0 t)\cos(\omega t) + \omega R_{rot} t \sin(\omega t), \tag{7a}$$

$$y(t) = -(R_{rot} + v_0 t)\sin(\omega t) + \omega R_{rot} t \cos(\omega t), \tag{7b}$$

$$v(t) = \sqrt{(v_0 + \omega^2 R_{rot} t)^2 + (\omega v_0 t)^2}, \tag{7c}$$

where s and t are related by $v = ds/dt$. A solution is presented in Fig. 2.

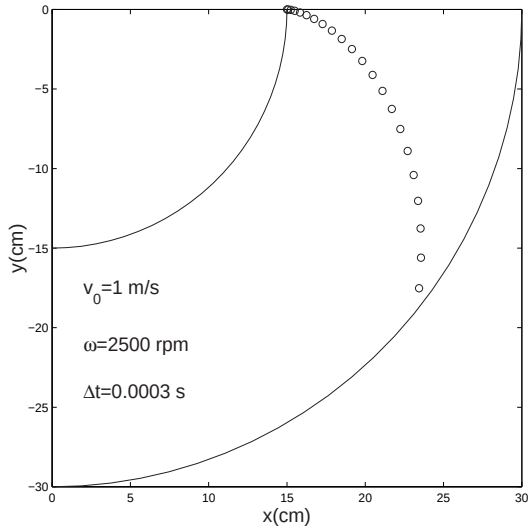

FIGURE 2. Spinning line without viscous forces

Realistic values for the physical parameters are in the viscous case:

$$\rho = 1700 \quad kg/m^3, \qquad \eta = 1200 \quad Pa\,s, \qquad v_0 = 1 \quad m/s,$$

$$R_{rot} = 0.15 \quad m, \qquad R_{coag} = 0.3 \quad m, \qquad A(0) = \pi/64\ 10^{-6} \quad m^2.$$

Originally, it was decided to use shooting techniques for system (2-5) with appropriate choices for F_0 in (6). The differential equations were solved by a routine for stiff systems from the NAG-library. However, difficulties arose as the solution appeared to be extremely sensitive to the choice for the initial viscous force. In many cases the solution became unstable and sometimes the spinning line moved in the wrong direction.

3. Numerical solution methods

The system of 2 second-order and 2 first-order differential equations (2-5) could be discretized as a boundary-value problem on the interval $[0, L]$, where the value of L is yet unknown. This approach, however, would involve some programming effort, resulting in a large system of nonlinear equations, which had to be solved several times to find an appropriate value for L. Moreover, it was not a priori clear how to choose the grid points, as we suspected that an equidistant grid would not do. Therefore we deemed this approach not to be feasible within the limited time available, and beyond that, in case of failure the intrinsic difficulty in the model would not be revealed.

We then decided to split the system into two parts, such that each could be solved in a straightforward manner. The second-order equations for x and y, (2-3) can be solved by an integration method when F and v are known. Once x and y are known, a boundary-value technique could be applied to solve the second-order system for v,

$$\frac{\eta}{\rho}\left(-\frac{d^2v}{ds^2}+\frac{1}{v}\left(\frac{dv}{ds}\right)^2\right)+v\frac{dv}{ds}=\omega^2\left(x\frac{dx}{ds}+y\frac{dy}{ds}\right), \tag{8}$$

which is obtained by substitution of (4) into (5). For simplicity, we impose here a Neumann boundary condition at $s = L$

$$\frac{dv}{ds}=0, \quad (s=L).$$

To start with, we solve the non-viscous model ($\eta = 0$) which has the known solution given by (7). Thereafter, we alternate solving system (2-3) and equation (8) using a Picard-iteration, with the idea that this process might converge to the solution of the complete system (2-5). In doing so, we encountered several problems.

First, observe that the second derivatives in (2-3) are multiplied by the factor $F - \Phi v$, so the system becomes singular whenever this factor changes sign, and the solution will explode. This phenomenon does not occur for small values of the viscosity η, as F is then small too. However, increasing the viscosity a value of η is reached for which the system (2-3) could not be solved anymore. Meanwhile, in discussions during the workshop, doubt arose about the validity of the initial condition involving the direction of the velocity, given by (6b), in the non-viscous case. Therefore, we decided to replace these conditions by

$$\frac{dy}{ds}=v_y, \qquad \frac{dx}{ds}=\sqrt{1-v_y^2}, \tag{9}$$

and tried to apply the Picard-iteration for several values of v_y. It appeared that this change of the direction of the spinning line at the orifice had a stabilizing effect on the solution of the system. Moreover,

the success of the Picard-iteration was very sensitive to the choice of the angle, determined by v_y, at the orifice (see Table 3). The quotient

η/ρ	v_y	result
0.001	0	4 iterations successfull
0.01	0	unstable
	-0.1	4 iterations successfull
	-0.2	unstable
0.1	-0.1	unstable
	-0.4	1 iteration successfull
0.2	-0.45	1 iteration successfull
0.3	-0.5	1 iteration successfull
0.4	-0.5	1 iteration successfull
0.5	-0.5	1 iteration successfull
0.7	-0.5	wrong trajectory
	-0.6	1 iteration successfull
	-0.7	1 iteration successfull

TABLE 3. Influence of η/ρ and v_y on Picard iteration

0.7 is derived from the physical values of the parameters. We present the trajectories obtained after 1 Picard-iteration for the starting values $v_y = -0.5$ and $v_y = -0.7$ in Fig. 3. It was possible to apply a

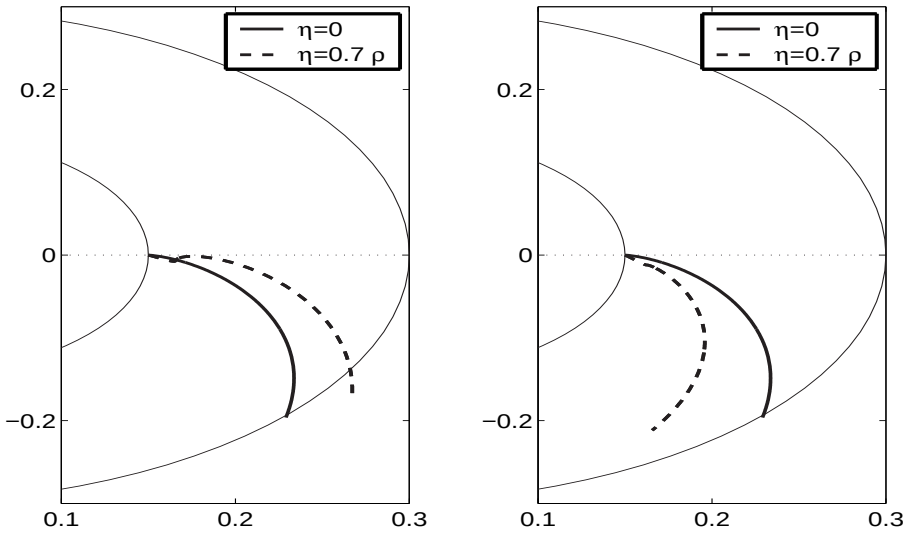

FIGURE 3. Trajectories for $v_y = -0.5$ (left) and $v_y = -0.7$ (right)

Picard-iteration in case of the initial condition $v_y = -0.5$, the resulting trajectory, however, appears to be nonphysical. We conclude that

both the solution process and the resulting trajectory are very sensitive to the choice of the initial conditions, and that some effort might be required to establish correct ones.
Secondly, we observed that the solution of the system (2-5) does not satisfy the condition (1) in the initial phase of the integration. Although (2-5) is mathematically equivalent to the original system (1-4) the numerical solutions are not, and guard must be taken that the deviation from (1) is not too strong. In a second experiment we solved the initial phase of (2-5), using the Runge-Kutta order four method with a very small step-size h, and measured the deviation from condition (1). Table 4 shows the results for several initial conditions.

F_0/Φ	$v_y = 0$	$v_y = -0.1$	$v_y = -0.2$	$v_y = -0.3$	$v_y = -0.4$	$v_y = -0.5$
0.5	$6.8_{10^{-8}}$	$6.3_{10^{-8}}$	$5.7_{10^{-7}}$	$1.6_{10^{-6}}$	$3.0_{10^{-6}}$	$4.7_{10^{-6}}$
0.7	$6.2_{10^{-7}}$	$5.8_{10^{-7}}$	$5.3_{10^{-6}}$	$1.5_{10^{-5}}$	$2.9_{10^{-5}}$	$4.7_{10^{-5}}$
0.9	$4.0_{10^{-5}}$	$3.7_{10^{-5}}$	$3.6_{10^{-4}}$	$1.0_{10^{-3}}$	$2.3_{10^{-3}}$	$4.3_{10^{-3}}$
1.1	unstable	unstable	unstable	unstable	$5.8_{10^{-2}}$	$1.1_{10^{-2}}$
1.3	unstable	unstable	$2.0_{10^{-1}}$	$1.7_{10^{-2}}$	$3.4_{10^{-3}}$	$9.2_{10^{-4}}$
1.5	$8.9_{10^{-1}}$	$3.7_{10^{-1}}$	$1.5_{10^{-2}}$	$5.1_{10^{-3}}$	$1.5_{10^{-3}}$	$5.0_{10^{-4}}$

TABLE 4. Maximum of $1 - \|[\frac{dx}{ds}, \frac{dy}{ds}]\|$ in the first 5 integration steps, $h = 10^{-5}$

Notwithstanding the small step size, condition (1) is severely violated in case v_y=0 and $F_0 > \Phi$, whereas we observe improvement for larger (negative) values for v_y. Again, we conclude that nonzero initial conditions for dy/ds should be considered. Moreover, it seems worth while to write the equations (2-3) in conservation form, using (5),

$$(10a) \quad (F - \Phi v)\frac{d^2x}{ds^2} = \frac{\Phi\omega^2}{v}\frac{dy}{ds}\left(y\frac{dx}{ds} - x\frac{dy}{ds}\right) - 2\Phi\omega\frac{dy}{ds},$$

$$(10b) \quad (F - \Phi v)\frac{d^2y}{ds^2} = -\frac{\Phi\omega^2}{v}\frac{dx}{ds}\left(y\frac{dx}{ds} - x\frac{dy}{ds}\right) + 2\Phi\omega\frac{dx}{ds},$$

and use an integration method which preserves conservation. Preliminary calculations indicate that the Runge-Kutta method does not become unstable for system (10) together with (4-5), although the accuracy is low in the case $F_0/\Phi = 1.1$. As an alternative, one might consider solving the differential algebraic system (1-4). In any case, the trajectory near the orifice is extremely sensitive to perturbations.

4. Analytical results

First we eliminate the viscous force F from the equations (2-3), and then the system is rewritten using $v = ds/dt$ to equations with time t

as independent variable, yielding

$$\begin{aligned}
\frac{d^2x}{dt^2} - \omega^2 x - 2\omega\frac{dy}{dt} &= \frac{\eta}{\rho}\frac{d}{dt}\left(\frac{1}{v^3}\frac{dv}{dt}\frac{dx}{dt}\right), \\
\frac{d^2y}{dt^2} - \omega^2 y + 2\omega\frac{dx}{dt} &= \frac{\eta}{\rho}\frac{d}{dt}\left(\frac{1}{v^3}\frac{dv}{dt}\frac{dy}{dt}\right), \\
\left(\frac{dx}{dt}\right)^2 + \left(\frac{dy}{dt}\right)^2 &= v^2.
\end{aligned}$$

Now, the variables x, y, v and t will be rescaled

$$\begin{aligned}
\tilde{t} &= \omega t, \quad v = \omega R_{rot}\tilde{v}, \\
x &= R_{rot}\tilde{x}, \quad y = R_{rot}\tilde{y},
\end{aligned}$$

so the equations become dimensionless. Eliminating $\tilde{v}$, dropping the $\tilde{}$ for convenience and denoting the differentiation with respect to t by $'$ yields the singularly perturbed system

$$x'' - x - 2y' = \frac{\eta}{\rho\omega R_{rot}^2}\left(\frac{(x'x'' + y'y'')\,x'}{(x'x' + y'y')^2}\right)', \tag{11a}$$

$$y'' - y + 2x' = \frac{\eta}{\rho\omega R_{rot}^2}\left(\frac{(x'x'' + y'y'')\,y'}{(x'x' + y'y')^2}\right)'. \tag{11b}$$

The initial conditions read

$$x = 1, \quad y = 0, \quad x' = \frac{v_0}{\omega R_{rot}}, \quad y' = 0,$$

and the boundary conditions at (unkown) time $t = T$

$$x(T)^2 + y(T)^2 = \frac{R_{coag}}{R_{rot}} = 4, \quad [x'(T), y'(T)] \cdot [x(T), y(T)] = 0, \cdots .$$

For the practical application we introduce the small parameters

$$\epsilon = \frac{\eta}{\rho\omega R_{rot}^2} \approx 0.12, \quad \delta = \frac{v_0}{\omega R_{rot}} \approx 0.026.$$

Then, the perturbed system reads in operator form

$$L\mathbf{u} = \epsilon\mathbf{f}(\mathbf{u}) \tag{12}$$

together with boundary conditions (BC's), and as a first step we might approximate the solution $\mathbf{u} = [x, y]$ by the regular perturbation expansion

$$\mathbf{u} = \mathbf{u_0} + \epsilon\mathbf{u_1} + \cdots ,$$

where $\mathbf{u_0}$ and $\mathbf{u_1}$ satisfy the boundary value problems

$$\begin{aligned}
L\mathbf{u_0} &= \mathbf{0}, \quad \text{(inhomogeneous BC's)}\,, \\
L\mathbf{u_1} &= \mathbf{f}(\mathbf{u_0}), \quad \text{(homogeneous BC's)}\,.
\end{aligned}$$

The solution for the first problem gives the bullet trajectory (cf. (7))

$$x_0(t) = (1+\delta t)cos(t) + tsin(t), \quad y_0(t) = -(1+\delta t)sin(t) + tcos(t),$$

The second problem is solved using Maple for various combinations of δ and ϵ. Fig. 4 shows the trajectories determined by $\mathbf{u_0}$ and $\mathbf{u_0} + \epsilon\mathbf{u_1}$ for $\delta = 0.025$ and $\epsilon = 0.0005$. The value for ϵ is non physical, but the plot clearly shows that even a small viscosity leads to an unacceptable trajectory near the rotor, probably due to the condition $y' = 0$ and to the existence of a boundary layer near the rotor.

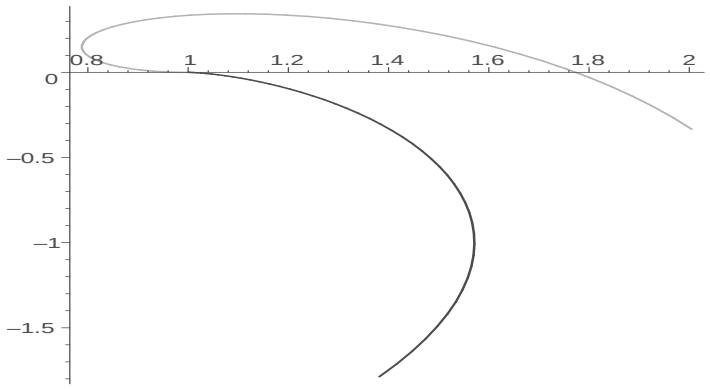

FIGURE 4. Trajectories for $\delta = 0.025, \epsilon = 0.0005$

Acceptable trajectories are obtained for values of δ not close to zero, even if the viscosity is large, as is shown in Fig. 5 (left), obtained for $\delta = \epsilon = 1$. In case of physical values for δ and ϵ it turned out to

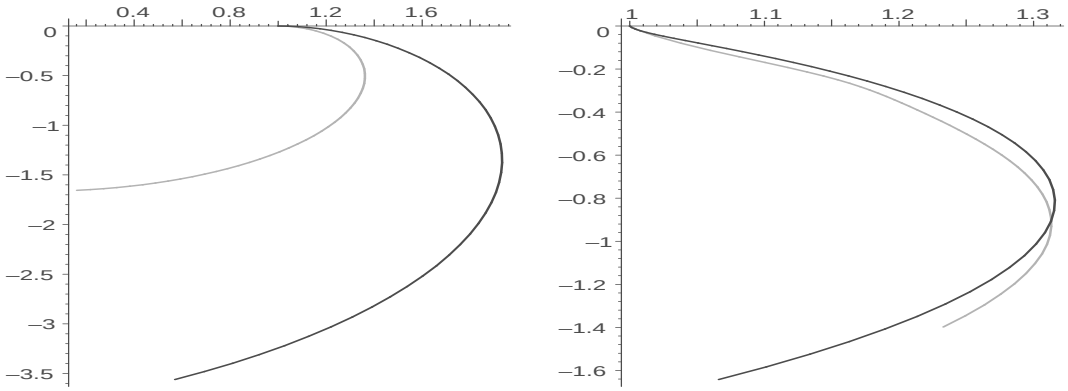

FIGURE 5. Trajectories for $\delta = 1, \epsilon = 1$ and for $\delta = 0.025, \epsilon = 0.12, y' = -sin(\pi/18)$.

be impossible to obtain satisfactory results, using $y' = 0$. However, negative angles for the trajectory at the rotor, i.e. $y' < 0$ had a stabilizing effect. In Fig. 5 (right) the results are shown for $\delta = 0.025, \epsilon =$

$0.12, y' = -sin(\pi/18)$. These results indicate again that the behavior of the solution near the rotor should be reconsidered.
System (12) can be considered as a singularly perturbed problem with a boundary layer most likely near the rotor. As a second step we could apply singular perturbation techniques in this layer. We rescale the dimensionless equations (11) near $t = 0$ by

$$x = 1 + \epsilon^{\alpha}\overline{x}, \quad y = \epsilon^{\beta}\overline{y}, \quad t = \epsilon^{\gamma}\overline{t}.$$

Interesting values for the parameters turn out to be $\alpha = \gamma = 1, \beta = 2$. Collecting the lowest order terms then gives

$$\begin{aligned} \frac{d^2\overline{x}}{d\overline{t}^2} &= \frac{d}{d\overline{t}}\left(\frac{1}{w^2}\frac{d^2\overline{x}}{d\overline{t}^2}\right), \quad w = \frac{d\overline{x}}{d\overline{t}}, \\ \frac{d^2\overline{y}}{d\overline{t}^2} + 2\frac{d\overline{x}}{d\overline{t}} &= \frac{d}{d\overline{t}}\left(\frac{1}{w^3}\frac{d^2\overline{x}}{d\overline{t}^2}\frac{d\overline{y}}{d\overline{t}}\right). \end{aligned}$$

Solving these equations will give an approximation to the trajectory in the boundary layer near the orifice. For other parts of the trajectory a similar approach, using different scalings, could be applied, and then the obtained solutions could be matched.

5. Time-dependent model

In the time-dependent description, the coordinates are r, the distance to the axis of the rotor, and t, the time. We introduce θ as the angle between the x-axis and the position vector $\boldsymbol{x}$ of the fluid,

$$\mathbf{x} = r\,(cos(\theta), sin(\theta))^T, \tag{13}$$

and we denote the velocity vector by $\mathbf{v}$. Further we introduce the *rotation matrix* J

$$J = \begin{pmatrix} 0 & -1 \\ 1 & 0 \end{pmatrix},$$

so that the tangent vector and its length are given by

$$\frac{\partial \boldsymbol{x}}{\partial r} = \left(\frac{1}{r}I + \frac{\partial\theta}{\partial r}J\right)\boldsymbol{x}, \quad \left|\frac{\partial \boldsymbol{x}}{\partial r}\right| = \sqrt{1 + r^2\left(\frac{\partial\theta}{\partial r}\right)^2},$$

The normalized tangent vector $\boldsymbol{t}$ and the unit normal vector $\boldsymbol{n}$ are

$$\boldsymbol{t} = \frac{1}{|\partial\boldsymbol{x}/\partial r|}\frac{\partial\boldsymbol{x}}{\partial r}, \tag{14}$$

$$\boldsymbol{n} = J\boldsymbol{t}. \tag{15}$$

5.1. Fixed coordinate system. First we derive the time derivative of the angle θ from the fact that the fluid moves with flow velocity $\boldsymbol{v}$. The equation

$$\left(\boldsymbol{v} - \frac{\partial \boldsymbol{x}}{\partial t}\right) \cdot \boldsymbol{n} = 0,$$

then leads to, using (13) and (15),

$$\frac{\partial \theta}{\partial t} = \frac{\boldsymbol{v} \cdot \boldsymbol{n}}{\boldsymbol{x} \cdot \boldsymbol{t}}. \tag{16}$$

The other time derivatives, for A and for $\boldsymbol{v}$, will be found from the balances of mass (continuity equation) and momentum. However, we will first derive a general conservation law in a segment between the coordinates $r = R_1$ and $r = R_2$ for a local quantity d transported with flux $\boldsymbol{f}$ (see Fig. 6)

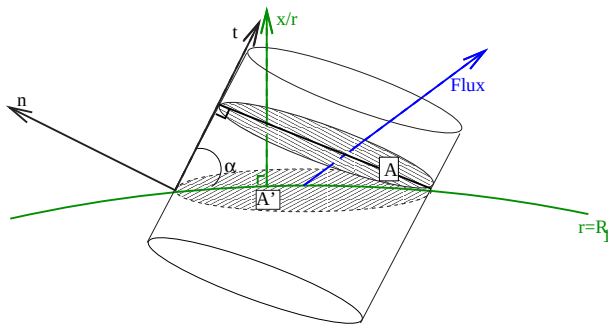

FIGURE 6. Transport passes through the 'skewed' cross-section A'.

$$\frac{\partial}{\partial t} \int_{R_1}^{R_2} Ad \left|\frac{\partial \boldsymbol{x}}{\partial r}\right| \, \mathrm{d}r + \left[\frac{\boldsymbol{x} \cdot \boldsymbol{f}}{\boldsymbol{x} \cdot \boldsymbol{t}} A\right]_{R_1}^{R_2} = 0.$$

Because this equation holds for every R_1 and R_2, we obtain the general conservation law in differential form (if the solution is sufficiently smooth):

$$\frac{\partial}{\partial t}\left(Ad\left|\frac{\partial \boldsymbol{x}}{\partial r}\right|\right) + \frac{\partial}{\partial r}\left(\frac{\boldsymbol{x} \cdot \boldsymbol{f}}{\boldsymbol{x} \cdot \boldsymbol{t}} A\right) = 0. \tag{17}$$

The continuity equation is obtained by applying (17) to mass with density $d = \rho$ and flux $\boldsymbol{f} = \rho \boldsymbol{v}$:

$$\frac{\partial}{\partial t}\left(\rho A\left|\frac{\partial \boldsymbol{x}}{\partial r}\right|\right) + \frac{\partial}{\partial r}\left(\rho A \frac{\boldsymbol{x} \cdot \boldsymbol{v}}{\boldsymbol{x} \cdot \boldsymbol{t}}\right) = 0 \tag{18}$$

The momentum equations for the x and y components of the velocity are found by applying (17) to momentum, e.g. for the x-component

$$d = \rho u, \qquad \boldsymbol{f} = \rho u \boldsymbol{v} - (1,0) T_{visc},$$

where the viscosity tensor is given by

$$T_{visc} = \frac{\eta}{|\partial \boldsymbol{x}/\partial r|} \left(\boldsymbol{t} \cdot \frac{\partial \boldsymbol{v}}{\partial r} \right) \boldsymbol{t}\boldsymbol{t}^T.$$

These equations read in vector form

$$\frac{\partial}{\partial t} \left(\rho A \boldsymbol{v} \left| \frac{\partial \boldsymbol{x}}{\partial r} \right| \right) + \frac{\partial}{\partial r} \left(\rho A \boldsymbol{v} \frac{\boldsymbol{x} \cdot \boldsymbol{v}}{\boldsymbol{x} \cdot \boldsymbol{t}} - \frac{\eta A}{|\partial \boldsymbol{x}/\partial r|} \left(\boldsymbol{t} \cdot \frac{\partial \boldsymbol{v}}{\partial r} \right) \boldsymbol{t} \right) = 0. \tag{19}$$

An equation for the kinetic energy,

$$E = \frac{1}{2} \rho A |\boldsymbol{v}|^2,$$

may be derived from

$$\frac{\partial}{\partial t} \left(\left| \frac{\partial \boldsymbol{x}}{\partial r} \right| E \right) = \boldsymbol{v} \cdot \frac{\partial}{\partial t} \left(\rho A \left| \frac{\partial \boldsymbol{x}}{\partial r} \right| \boldsymbol{v} \right) - \frac{1}{2} |\boldsymbol{v}|^2 \frac{\partial}{\partial t} \left(\rho A \left| \frac{\partial \boldsymbol{x}}{\partial r} \right| \right).$$

Substituting the continuity equation (18) and momentum equations (19), and combining advection and viscous terms yields

$$\frac{\partial}{\partial t} \left(\left| \frac{\partial \boldsymbol{x}}{\partial r} \right| E \right) + \frac{\partial}{\partial r} \left(E \frac{\boldsymbol{x} \cdot \boldsymbol{v}}{\boldsymbol{x} \cdot \boldsymbol{t}} - \frac{1}{2} \frac{\eta A}{|\partial \boldsymbol{x}/\partial r|} \boldsymbol{t}^T \frac{\partial \boldsymbol{v}\boldsymbol{v}^T}{\partial r} \boldsymbol{t} \right) = - \frac{\eta A}{|\partial \boldsymbol{x}/\partial r|} \left(\boldsymbol{t} \cdot \frac{\partial \boldsymbol{v}}{\partial r} \right)^2. \tag{20}$$

5.2. Rotating coordinate system. Stationary solutions can only be found on a rotating coordinate system. The transformation is obtained by choosing the variable $\tilde{\theta} := \theta - \omega t$, where ω is the angular speed of the rotor. In the derivation of the transformed equations we will frequently use the rotation matrix

$$C = \begin{pmatrix} \cos(\omega t) & -\sin(\omega t) \\ \sin(\omega t) & \cos(\omega t) \end{pmatrix}$$

The transformed position vector $\tilde{\boldsymbol{x}}$ is given by

$$\tilde{\boldsymbol{x}} = r \left(\cos(\tilde{\theta}), \sin(\tilde{\theta}) \right)^T, \tag{21}$$

which relates to the original coordinates by

$$\boldsymbol{x} = C \tilde{\boldsymbol{x}}.$$

The partial derivatives of $\boldsymbol{x}$ satisfy

$$\frac{\partial \boldsymbol{x}}{\partial r} = C \frac{\partial \tilde{\boldsymbol{x}}}{\partial r}, \quad \frac{\partial \boldsymbol{x}}{\partial t} = C \left(\frac{\partial \tilde{\boldsymbol{x}}}{\partial t} + \omega J \tilde{\boldsymbol{x}} \right).$$

The velocity $\boldsymbol{v}$ and the unit tangent and normal vectors can be expressed in the transformed coordinates, too:

$$\boldsymbol{t} = C\tilde{\boldsymbol{t}}, \quad \boldsymbol{n} = C\tilde{\boldsymbol{n}}, \quad \boldsymbol{v} = C\left(\tilde{\boldsymbol{v}} + \omega J\tilde{\boldsymbol{x}}\right).$$

As a consequence, the dot products satisfy

$$\boldsymbol{x}\cdot\boldsymbol{v} = \tilde{\boldsymbol{x}}\cdot\tilde{\boldsymbol{v}}, \quad \boldsymbol{x}\cdot\boldsymbol{t} = \tilde{\boldsymbol{x}}\cdot\tilde{\boldsymbol{t}}, \quad \boldsymbol{t}\cdot\frac{\partial\boldsymbol{v}}{\partial r} = \tilde{\boldsymbol{t}}\cdot\frac{\partial\tilde{\boldsymbol{v}}}{\partial r}.$$

The kinematic equation now reads in the new coordinate system, using the fact that both J and C are orthogonal matrices,

$$\frac{\partial\tilde{\theta}}{\partial t} + \omega = \frac{(C\tilde{\boldsymbol{v}} + \omega CJ\tilde{\boldsymbol{x}})\cdot(C\tilde{\boldsymbol{n}})}{\tilde{\boldsymbol{x}}\cdot\tilde{\boldsymbol{t}}} = \frac{\tilde{\boldsymbol{v}}\cdot\tilde{\boldsymbol{n}}}{\tilde{\boldsymbol{x}}\cdot\tilde{\boldsymbol{t}}} + \omega. \tag{22}$$

The transformed continuity equation becomes

$$\frac{\partial}{\partial t}\left(\rho A\left|\frac{\partial\tilde{\boldsymbol{x}}}{\partial r}\right|\right) + \frac{\partial}{\partial r}\left(\rho A\frac{\tilde{\boldsymbol{x}}\cdot\tilde{\boldsymbol{v}}}{\tilde{\boldsymbol{x}}\cdot\tilde{\boldsymbol{t}}}\right) = 0. \tag{23}$$

The derivation of the transformed momentum equation is slightly more complicated. First, we express each of the terms in (19) in the transformed variables.

$$\begin{aligned}
\frac{\partial}{\partial t}\left(\rho A\boldsymbol{v}\left|\frac{\partial\boldsymbol{x}}{\partial r}\right|\right) &= C\frac{\partial}{\partial t}\left(\rho A\tilde{\boldsymbol{v}}\left|\frac{\partial\tilde{\boldsymbol{x}}}{\partial r}\right|\right) + \omega CJ\tilde{\boldsymbol{x}}\frac{\partial}{\partial t}\left(\rho A\left|\frac{\partial\tilde{\boldsymbol{x}}}{\partial r}\right|\right) + \\
&\quad + \omega CJ\rho A\left|\frac{\partial\tilde{\boldsymbol{x}}}{\partial r}\right|\frac{\partial\tilde{\boldsymbol{x}}}{\partial t} + \rho A\left|\frac{\partial\tilde{\boldsymbol{x}}}{\partial r}\right|\frac{\partial C}{\partial t}\left(\tilde{\boldsymbol{v}} + \omega J\tilde{\boldsymbol{x}}\right), \\
\frac{\partial}{\partial r}\left(\rho A\boldsymbol{v}\frac{\boldsymbol{x}\cdot\boldsymbol{v}}{\boldsymbol{x}\cdot\boldsymbol{t}}\right) &= C\frac{\partial}{\partial r}\left(\rho A\tilde{\boldsymbol{v}}\frac{\tilde{\boldsymbol{x}}\cdot\tilde{\boldsymbol{v}}}{\tilde{\boldsymbol{x}}\cdot\tilde{\boldsymbol{t}}}\right) + \omega CJ\tilde{\boldsymbol{x}}\frac{\partial}{\partial r}\left(\rho A\frac{\tilde{\boldsymbol{x}}\cdot\tilde{\boldsymbol{v}}}{\tilde{\boldsymbol{x}}\cdot\tilde{\boldsymbol{t}}}\right) + \\
&\quad + \omega CJ\rho A\frac{\tilde{\boldsymbol{x}}\cdot\tilde{\boldsymbol{v}}}{\tilde{\boldsymbol{x}}\cdot\tilde{\boldsymbol{t}}}\frac{\partial\tilde{\boldsymbol{x}}}{\partial r},
\end{aligned}$$

and

$$-\frac{\partial}{\partial r}\left(\frac{\eta A}{|\partial\boldsymbol{x}/\partial r|}\left(\boldsymbol{t}\cdot\frac{\partial\boldsymbol{v}}{\partial r}\right)\boldsymbol{t}\right) = -C\frac{\partial}{\partial r}\left(\frac{\eta A}{|\partial\tilde{\boldsymbol{x}}/\partial r|}\left(\tilde{\boldsymbol{t}}\cdot\frac{\partial\tilde{\boldsymbol{v}}}{\partial r}\right)\tilde{\boldsymbol{t}}\right).$$

Combining these terms and using the transformed continuity equation leads to

$$\begin{aligned}
C\ &\frac{\partial}{\partial t}\left(\rho A\tilde{\boldsymbol{v}}\left|\frac{\partial\tilde{\boldsymbol{x}}}{\partial r}\right|\right) + C\frac{\partial}{\partial r}\left(\rho A\tilde{\boldsymbol{v}}\frac{\tilde{\boldsymbol{x}}\cdot\tilde{\boldsymbol{v}}}{\tilde{\boldsymbol{x}}\cdot\tilde{\boldsymbol{t}}}\right) - C\frac{\partial}{\partial r}\left(\frac{\eta A}{|\partial\boldsymbol{x}/\partial r|}\left(\tilde{\boldsymbol{t}}\cdot\frac{\partial\tilde{\boldsymbol{v}}}{\partial r}\right)\tilde{\boldsymbol{t}}\right) + \\
&+\rho A\left|\frac{\partial\tilde{\boldsymbol{x}}}{\partial r}\right|\frac{\partial C}{\partial t}\left(\tilde{\boldsymbol{v}} + \omega J\tilde{\boldsymbol{x}}\right) + \omega CJ\rho A\left|\frac{\partial\tilde{\boldsymbol{x}}}{\partial r}\right|\frac{\partial\tilde{\boldsymbol{x}}}{\partial t} + \omega CJ\rho A\frac{\tilde{\boldsymbol{x}}\cdot\tilde{\boldsymbol{v}}}{\tilde{\boldsymbol{x}}\cdot\tilde{\boldsymbol{t}}}\frac{\partial\tilde{\boldsymbol{x}}}{\partial r} = 0.
\end{aligned}$$

Now, observe that

$$\frac{\partial\boldsymbol{C}}{\partial t} = \omega CJ, \quad \frac{\partial\tilde{\boldsymbol{x}}}{\partial t} = J\tilde{\boldsymbol{x}}\frac{\partial\tilde{\theta}}{\partial t}.$$

Rearranging terms, and pre-multiplication by C^{-1} then yields

$$\begin{aligned}
&\frac{\partial}{\partial t}\left(\rho A\tilde{\boldsymbol{v}}\left|\frac{\partial\tilde{\boldsymbol{x}}}{\partial r}\right|\right)+\frac{\partial}{\partial r}\left(\rho A\tilde{\boldsymbol{v}}\frac{\tilde{\boldsymbol{x}}\cdot\tilde{\boldsymbol{v}}}{\tilde{\boldsymbol{x}}\cdot\tilde{\boldsymbol{t}}}-\frac{\eta A}{|\partial\boldsymbol{x}/\partial r|}\left(\tilde{\boldsymbol{t}}\cdot\frac{\partial\tilde{\boldsymbol{v}}}{\partial r}\right)\tilde{\boldsymbol{t}}\right)\\
&\quad= -\rho A\left|\frac{\partial\tilde{\boldsymbol{x}}}{\partial r}\right|\omega\left(J\tilde{\boldsymbol{v}}+\omega J^2\tilde{\boldsymbol{x}}+J^2\tilde{\boldsymbol{x}}\frac{\tilde{\boldsymbol{v}}\cdot\tilde{\boldsymbol{n}}}{\tilde{\boldsymbol{x}}\cdot\tilde{\boldsymbol{t}}}+\frac{\tilde{\boldsymbol{x}}\cdot\tilde{\boldsymbol{v}}}{\tilde{\boldsymbol{x}}\cdot\tilde{\boldsymbol{t}}}J\tilde{\boldsymbol{t}}\right)\\
&\quad= -\rho A\left|\frac{\partial\tilde{\boldsymbol{x}}}{\partial r}\right|\omega\left(2J\tilde{\boldsymbol{v}}-\omega\tilde{\boldsymbol{x}}\right),
\end{aligned}$$

where we used (22), and the equalities

$$J^2=-I,\quad \tilde{\boldsymbol{n}}=J\tilde{\boldsymbol{t}},\quad \left(\tilde{\boldsymbol{x}}\cdot\tilde{\boldsymbol{t}}\right)J\tilde{\boldsymbol{v}}=\left(\tilde{\boldsymbol{x}}\cdot\tilde{\boldsymbol{v}}\right)J\tilde{\boldsymbol{t}}-\left(\tilde{\boldsymbol{v}}\cdot J\tilde{\boldsymbol{t}}\right)\tilde{\boldsymbol{x}}.$$

6. Conclusions

The viability might be questioned of the assumption that the solutions behave smoothly near the rotor. The initial condition $v_y = 0$ did lead to severe problems and non physical trajectories, both in the numerical experiments and in the regular perturbation. It has been suggested to first consider the problem of a polymer dropping down from a horizontal plate on a conveyer belt. Then, due to viscosity, the initial angle will not be perpendicular to the plate. The correct behavior near the plate might give a clue for the formulation of appropriate conditions in the rotor spinning problem.

Once correct boundary behavior has been obtained, it might very well be possible to solve the problem by clever shooting. However, care should be taken in the initial part of the trajectory, which is very sensitive to perturbations. Therefore we think that automatic shooting will fail, but trial and error by hand might be successful. In future research the models could be extended by including temperature effects and forces due to air friction.

Acknowledgement. We would like to thank Marc Peletier for his valuable contribution to our discussions.